Journal of the Korean Ceramic Society
Vol. 51, No. 4, pp. 278~282, 2014.

http://dx.doi.org/10.4191/kcers.2014.51.4.278

High Electrochemical Activity of Bi_2O_3-based Composite SOFC Cathodes

Woo Chul Jung, Yun-Jie Chang*, Kuan-Zong Fung*, and Sossina Haile,†**

Materials Science and Engineering, KAIST, Daejeon 305-701, Korea
**Materials Science and Engineering, NCKU, Tainan City 701, Taiwan*
***Materials Science, Caltech, Pasadena, CA 91125, USA*

(Received June 13, 2014; Revised July 22, 2014; Accepted July 23, 2014)

ABSTRACT

Due to high ionic conductivity and favorable oxygen electrocatalysis, doped Bi_2O_3 systems are promising candidates as solid oxide fuel cell cathode materials. Recently, several researchers reported reasonably low cathode polarization resistance by adding electronically conducting materials such as (La,Sr)MnO_3 (LSM) or Ag to doped Bi_2O_3 compositions. Despite extensive research efforts toward maximizing cathode performance, however, the inherent catalytic activity and electrochemical reaction pathways of these promising materials remain largely unknown. Here, we prepare a symmetrical structure with identically sized $Y_{0.5}Bi_{1.5}O_3$/LSM composite electrodes on both sides of a YSZ electrolyte substrate. AC impedance spectroscopy (ACIS) measurements of electrochemical cells with varied cathode compositions reveal the important role of bismuth oxide phase for oxygen electrocatalysis. These observations aid in directing future research into the reaction pathways and the site-specific electrocatalytic activity as well as giving improved guidance for optimizing SOFC cathode structures with doped Bi_2O_3 compositions.

Key words : Doped Bi_2O_3, Composite cathode, Oxygen reduction reaction, Impedance spectroscopy

1. Introduction

The ionic conductivity of certain doped Bi_2O_3 materials is reported to be one or two orders of magnitude higher than that of the doped ZrO_2 materials conventionally used as electrolytes in solid oxide fuel cells.[1] Moreover, doped Bi_2O_3 compositions are reported to have a favorable effect on the rate of oxygen electrocatalysis, making them promising candidates for cathode materials.[2-6] For example, the Liu group recently reported a reasonably low cathode polarization resistance of 0.3 Ω cm^2 at 600°C using a composite cathode consisting of silver and $Y_{0.5}Bi_{1.5}O_3$,[7] and the Wachsman group has reported a cathode polarization resistance of 0.43 Ω cm^2 at 600°C using a composite cathode consisting of $La_{1-x}Sr_xMnO_{3-\delta}$ (LSM) and $Er_{0.4}Bi_{1.6}O_3$.[8] However, the catalytic activity and mechanism of these promising materials are unknown, and thus it is also unknown how to design the material's microstructure so as to maximize cathode performance. Phase stability is also an important consideration; for example, upon long-term annealing at 600°C, $Y_xBi_{1-x}O_3$ and $Er_xBi_{1-x}O_3$ both exhibit a partial phase transition that leads to significant reduction in ionic conductivity.[9]

In this work, as a first step for optimizing the chemical composition and the microstructure of the Bi_2O_3 based composite cathode systems, we investigated the electrochemical activity of the doped Bi_2O_3 toward oxygen reduction reaction. Symmetrical structures with $Y_{0.5}Bi_{1.5}O_3$/LSM composite electrodes on both sides of a YSZ electrolyte substrate were prepared. AC impedance spectroscopy (ACIS) measurements of electrochemical cells with varied cathode compositions reveal the important role of bismuth oxide phase for oxygen electrocatalysis.

†Corresponding author : Sossina Haile
E-mail : smhaile@caltech.edu
Tel : +1-626-395-2958 Fax : +1-626-395-8868

2. Experimental Procedure

$Y_{0.5}Bi_{1.5}O_3$ (YB) powder was synthesized using a conventional solid state method, wherein the appropriate precursor oxides were mixed, calcined at 800°C for 5 h, and ball-milled for ~ 24 h followed by sieving through 200 mesh screen (particle sizes < ~ 600 nm). X-ray diffraction results obtained from the YB powder indicate that a single-phase fluorite was obtained.

Three composite YB-$La_{0.8}Sr_{0.2}MnO_3$ (LSM) cathode inks were prepared by mixing this in-house YB with commercial LSM (Fuelcellmaterials, 121101, 5 - 8 m^2/g specific surface area and 0.7 - 1.1 mm particle size) in different weight ratios (YB : LSM = 50 : 50 wt%, 35 : 65 wt%, and 0 : 100 wt%). These compositions are hereafter referred to as YB50, YB35, and LSM. The powders were combined with a terpineol based organic vehicle (Fuel Cell Materials, 311006) at a powder loading of 70 wt% to obtain viscosities appropriate for brushing. Inks were applied by brush coating to each side of a $Y_{0.16}Zr_{0.84}O_{1.92}$ (YSZ) ceramic substrate (MTI, polycrystalline, YSZ101005SN) and dried at 80°C for 20 min.

After evaluating different firing conditions, a firing temperature of 850°C (5 h in air) was identified as suitable for the composite cathodes. In the case of neat LSM, the electrode slurry was sintered at 1200°C for 2 h in air. This higher temperature was chosen due to low sinterability and poor adhesion with a YSZ substrate at lower sintering temperatures. Gold paste (Fuelcellmaterials, AU-I-10) – a metal considered catalytically inert – was painted on the porous composite electrode surfaces to serve as a current collector.

The resulting symmetric cells were placed inside a continuous-flow alumina tube into which O_2 - Ar gas mixtures were delivered via digital mass flow controllers. The total flow rate was kept constant at 100 cm^3 min^{-1} (standard temperature and pressure), implying a gas velocity of 35.1 cm min^{-1} and both sides of the cell were exposed to the same gas environment. The electrochemical characteristics of the composite cathodes were measured by A.C. impedance spectroscopy (ACIS, Solartron 1260, perturbation voltage of 50 mV), carried out under controlled temperatures (500°C to 700°C) and atmospheres (pO_2 of 0.05 to 1 atm) under zero bias. Data were analyzed using ZView software (Scribner Associates, version 2.9b).

The microstructure and chemical composition were examined using a Carl Zeiss LEO 1550 VP scanning electron microscope (SEM), equipped with EDAX energy dispersive spectrometers (EDS).

3. Results and Discussion

3.1. Morphology characterization

SEM micrographs of the starting oxide powder are shown in Fig. 1. Both powders have particle sizes ranging from less than one micron to a few microns. The $Y_{0.5}Bi_{1.5}O_3$ particles appear smaller and rounder than the LSM particles. According to the LSM vendor, the LSM powder has a specific surface area of 5-8 m^2/g and a particle size (d50) of 0.7-1.1 mm.

Figure 2 shows SEM images of three YB–LSM composite layers (weight ratio of 1 : 1) fired at different temperatures for 2 h. Although the view of the composite electrode is slightly obscured by the Au current collector, it appears the LSM particles are not fully interconnected after firing at 850°C for 2 h. At a somewhat higher firing temperature (1050°C) the YB particles appear to become isolated. Upon firing at 1200°C the YB particles adopt a rod-like form, indicative of melting and recrystallization (Fig. 2(c)). To obtain high porosity and small grains, and prevent the YB particles from melting, in this initial study a firing temperature of 850°C and duration of 5 h were chosen for fabricating composite cathodes.

Cross-sectional SEM images of the three samples, collected after the ACIS measurements, are shown in Fig. 3. Highly porous, 10 mm thick composite layers were obtained for both YB50 and YB35; the pure LSM electrode was slightly more compact (7 mm thickness) and appeared to have larger feature sizes, consistent with the higher firing temperature used for that electrode. EDS mapping was used to identify which particles are YB and which are LSM,

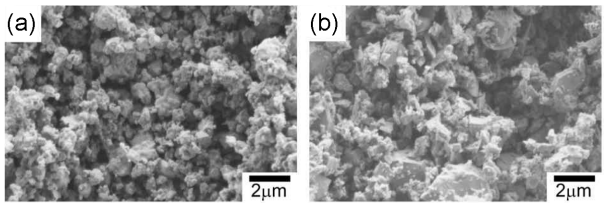

Fig. 1. SEM micrographs of oxide powder. (a) $Y_{0.5}Bi_{1.5}O_3$ and (b) $La_{0.8}Sr_{0.2}MnO_3$.

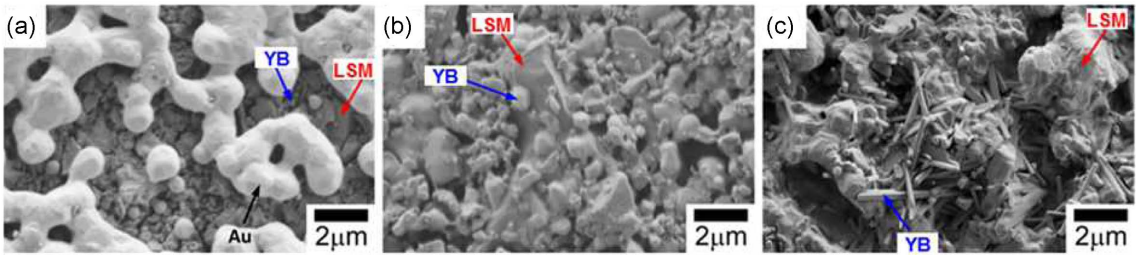

Fig. 2. SEM micrographs of three YB–LSM composite species (weight ratio of 1 : 1) fired at 850°C, 1050°C, and 1200°C, respectively for 2 h in air.

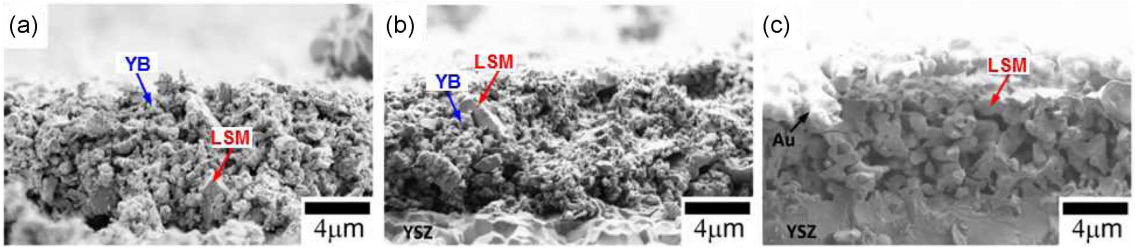

Fig. 3. Cross-sectional SEM images of the three composite electrodes with different compositions used for the ACIS measurements. (a) YB : LSM = 50 : 50 wt% (YB50), (b) YB : LSM = 35 : 65 wt% (YB35), and (c) YB : LSM = 0 : 100 wt% (LSM).

and the results indicated that the LSM particles in the composite compositions are not well-connected**.** This lack of LSM interconnectivity and the poor electronic conductivity of YB suggest that catalysis will be limited to regions near the Au current collector. Note that no evidence of reaction between the YSZ electrolyte and the LSM cathode was observed, as expected from relatively low firing temperature used in this work.[10)]

3.2. Electrochemical impedance analysis

Selected results from the electrochemical impedance measurements are presented in Fig. 4. The raw impedance spectra exhibit an offset resistance (R_{off}, evident as a displacement of the data along the real axis) and two adjacent semicircles, one a nearly ideal arc at high frequencies and the other a somewhat distorted arc at low frequencies (Fig. 4(a)). The offset resistance is attributed to the YSZ bulk largely because it had, in all cases, an overall magnitude typical of ionic conductivity in YSZ. For the example shown (700°C), the implied conductivity is 4×10^{-3} S/cm, which is similar to the reported value of 1×10^{-2} S/cm at 650°C.[11)] Furthermore, the offset resistance was independent of electrode composition and pO_2 (Fig. 4(d)), as would be expected for the electrolyte. The activation energy of R_{off} of ~ 0.7 eV and a slight curvature in the Arrhenius plot (Fig. 4(c)) imply a minor contribution from sheet resistance

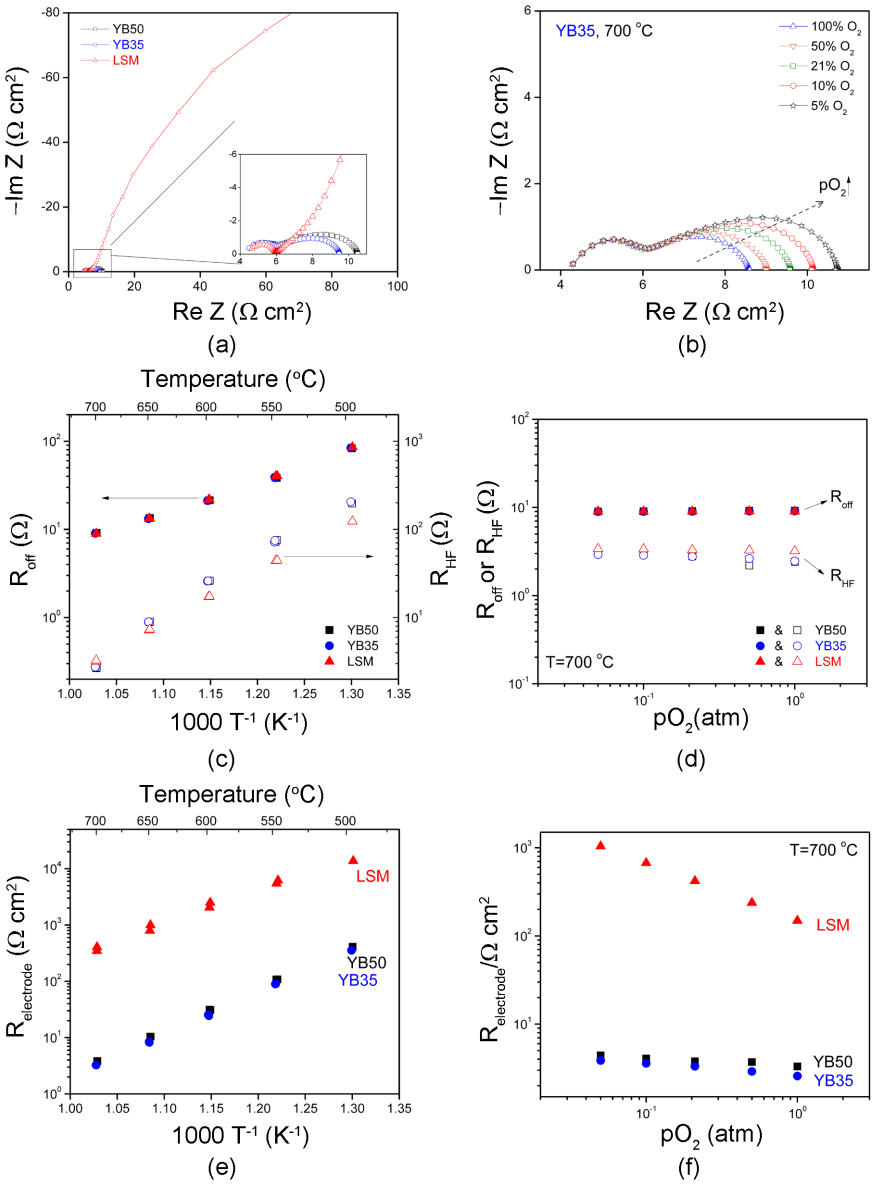

Fig. 4. (a) Typical impedance spectra obtained from Au | YB-LSM or LSM | YSZ | YB-LSM or LSM | Au symmetric cells at T = 700°C, pO_2 = 0.21 atm. (b) Impedanc spectra obtained from YB35 vs. pO_2 at 700°C (c) Arrhenius plot of the R_{off} and R_{HF} vs. temperature measured under pO_2 of 0.21 atm. (d) Double-logarithmic plots of R_{off} and R_{HF} vs. pO_2 measured at 700°C. (e) Arrhenius plot of $R_{electrode}$ (normalized by area) vs. temperature measured under pO_2 of 0.21 atm. (f) Double-logarithmic plots of $R_{electrode}$ (normalized by area) vs. pO_2 measured at 700°C.

Table 1. Values, Activation Energies and pO_2 Dependences of $R_{electrode}$ for Three Samples. $R_{electrode}$ Values were Obtained at 600 and 700°C under pO_2 of 0.21 atm. The pO_2 Dependences were Obatined by $R_{electrode}$ μ pO_2^{-m} (where m defines the power law dependence of log $R_{electrode}$ on pO_2).

Samples	$R_{electrode}$ / Ω cm^2 (600°C)	$R_{electrode}$ / Ω cm^2 (700°C)	E_a / eV	m
YB50	31	3.8	1.50 ± 0.01	0.08 – 0.10
YB35	24	3.3	1.50 ± 0.01	0.13 – 0.14
LSM	2500	410	1.17 ± 0.04	0.39 – 0.65

in the Au current collector. The high frequency arc resistance R_{HF} was also observed to be independent of electrode composition and pO_2, and its activation energy was measured as ~ 1.3 eV, which matches the grain boundary resistance typically observed in YSZ (Fig. 4(c) - (d)). Thus, it is only the distorted low frequency (LF) arc that is attributed to the YB-LSM electrode. Indeed, this arc exhibits substantial dependence on electrode composition and pO_2. Moreover, it exhibits relatively large capacitance values (e.g., 2.4×10^{-5} F/cm^2 for YB35 at 700°C, pO_2 of 0.21 atm), as expected for electrode behaviour.

Overall, the the area specific electrode polarization resistance $R_{electrode} = R_{LF}A/2$ (where A is the projected electrode area) of the YB-LSM composites is quite low and substantially smaller than that of neat LSM. For example, under air the composite polarization resistance is nearly 120 times smaller than it is in the neat LSM electrode. Furthermore, the two composite electrodes compositions exhibit nearly identical impedance behaviour and electrochemical activity. Table 1 summarizes the values and the activation energy of $R_{electrode}$, and the dependences of $R_{electrode}$ on pO_2^{-m} (where m defines the power law dependence of log $R_{electrode}$ on pO_2) for all three samples. The different activation energy and pO_2 dependence of $R_{electrode}$ between the composite and the pure LSM electrode suggest that the reduced electrode resistance is due not just to a difference in the number of catalytic sites, but also a difference in the activity of those sites, i.e., in the activity of YB. Further work, including a more quantitative approach to enable identification of reaction pathways and facilitate measurement of the site-specific electrocatalytic activity, is being initiated by the authors to address this interesting observation.

4. Conclusions

Exploratory measurements have been performed on bismuth oxide based composite cathodes consisting of $Y_{0.5}Bi_{1.5}O_3$ and $La_{0.8}Sr_{0.2}MnO_3$. Processing conditions for obtaining a porous, interconnected composite cathode structure onto a YSZ ceramic substrate were investigated in terms of composition and firing temperature. We demonstrated that YB is electrochemically active towards oxygen reduction by fabricating a symmetrical structure with YB/LSM composite electrodes on both sides of a YSZ electrolyte substrate and subsequently measuring AC Impedance Spectroscopy with varied cathode compositions. Surprisingly, the lowest electrode polarization resistance was obtained from a sample with the smallest amount of LSM phase, a state-of-the-art cathode catalyst, revealing the important role of bismuth oxide phase for oxygen electrocatalysis. The observation should aid in directing future research into the reaction pathways and the site-specific electrocatalytic activity as well as providing improved guidelines towards the development of composite cathodes with improved performance.

Acknowledgment

This work was carried out under the support of the Resnick Institute and the Taiwanese Ministry of Science and Technology under grant number NSC 103-3113-P-008-001. Additional support was provided by the Global Frontier R&D Program on Center for Multiscale Energy System funded by the National Research Foundation under the Ministry of Science, ICT & Future, Korea (2011-0031569).

REFERENCES

1. E. D. Wachsman and K. T. Lee, "Lowering the Temperature of Solid Oxide Fuel Cells," *Science*, **334** [6058] 935-39 (2011).
2. B. A. Boukamp, I. C. Vinke, K. J. Devries, and A. J. Burggraaf, "Surface Oxygen-exchange Properties of Bismuth Oxide-based Solid Electrolytes and Electrode Materials," *Solid State Ion.*, **32-33** [2] 918-23 (1989).
3. B. A. Boukamp, "Small Signal Response of the BiCuVOx/noble Metal/oxygen Electrode System," *Solid State Ion.*, **136** [SI] 75-82 (2000).
4. C. Y. Yoo, B. A. Boukamp, and H. J. M. Bouwmeester, "Oxygen Surface Exchange Kinetics of Erbia-stabilized Bismuth Oxide," *J. Solid State Electrochem.*, **15** [2] 231-36 (2011).
5. K. T. Lee, A. A. Lidie, S. Y. Jeon, G. T. Hitz, S. J. Song, and E. D. Wachsman, "Highly Functional Nano-scale Stabilized Bismuth Oxides via Reverse Strike Co-precipitation for Solid Oxide Fuel Cells," *J. Mater. Chem. A*, **1** [20] 6199-207 (2013).
6. R. D. Bayliss, S. N. Cook, S. Kotsantonis, R. J. Chater, and J. A. Kilner, "Oxygen Ion Diffusion and Surface Exchange Properties of the α- and δ-phases of Bi_2O_3," *Adv. Energy Mater.*, **4** [10] DOI : 10.1002/aenm.201301575 (2014).
7. C. Xia, Y. Zhang, and M. Liu, "Composite Cathode Based on Yttria Stabilized Bismuth Oxide for Low-temperature Solid Oxide Fuel Cells," *Appl. Phys. Lett.*, **82** [6] 901-03 (2003).

8. K. T. Lee, D. W. Jung, H. S. Yoon, A. A. Lidie, M. A. Camaratta, and E. D. Wachsman, "Interfacial Modification of $La_{0.80}Sr_{0.20}Mn_{3-d}$-$Er_{0.4}Bi_{0.6}O_3$ Cathodes for High Performance Lower Temperature Solid Oxide Fuel Cells," *J. Power Sources*, **220** 324-30 (2012).
9. K. Z. Fung and A. V. Virkar, "Phase-stability, Phase-transformation Kinetics, and Conductivity of Y_2O_3-Bi_2O_3 Solid Electrolytes Containing Aliovalent Dopants," *J. Am. Ceram. Soc.*, **74** [8] 1970-80 (1991).
10. Z. Jiang, L. Zhang, K. Feng, and C. Xia, "Nanoscale Bismuth Oxide Impregnated (La,Sr)MnO_3 Cathodes for Intermediate-temperature Solid Oxide Fuel Cells," *J. Power Sources*, **185** 40-48 (2008).
11. P. S. Manning, J. D. Sirman, R. A. DeSouza, and J. A. Kilner, "The Kinetics of Oxygen Transport in 9.5 mol % Single Crystal Yttria Stabilised Zirconia," *Solid State Ion.*, **100** [1-2] 1-10 (1997).